

NOTE: Ridge Formation and De-Spinning of Iapetus via an Impact-Generated Satellite

H. F. Levison¹, K. J. Walsh¹, A. C. Barr¹, L. Dones¹

¹Southwest Research Institute, 1050 Walnut St. Suite 300, Boulder, CO 80302, USA

Corresponding Author:
Harold F. Levison
hal@boulder.swri.edu
Southwest Research Institute
1050 Walnut St. Suite 300
Boulder, CO 80302, USA
1 (303) 546-0290

Abstract

We present a scenario for building the equatorial ridge and de-spinning Iapetus through an impact-generated disk and satellite. This impact puts debris into orbit, forming a ring inside the Roche limit and a satellite outside. This satellite rapidly pushes the ring material down to the surface of Iapetus, and then itself tidally evolves outward, thereby helping to de-spin Iapetus. This scenario can de-spin Iapetus an order of magnitude faster than when tides due to Saturn act alone, almost independently of its interior geophysical evolution. Eventually, the satellite is stripped from its orbit by Saturn. The range of satellite and impactor masses required is compatible with the estimated impact history of Iapetus.

1. Introduction

The surface and shape of Iapetus (with equatorial radius, $R_{\text{I}}=746$ km, and bulk density, $\bar{\rho} = 1.09$ g cm $^{-3}$) are unlike those of any other icy moon (Jacobson *et al.* 2006). About half of Iapetus’ ancient surface is dark, and the other half is bright (see Porco *et al.* 2005, for discussion). This asymmetry has been explained recently as the migration of water ice due to the deposition of darker material on the leading side of the body (Spencer and Denk 2010). Iapetus also has a ridge system near its equator, extending $> 110^\circ$ in longitude (Porco *et al.* 2005), that rises to heights of ~ 13 km in some locations (Giese *et al.* 2008). The ridge itself is heavily cratered, suggesting it originated during Iapetus’ early history. Finally, Iapetus’ present-day overall shape is consistent with a rapid 16-hour spin period rather than its present 79-day spin period (Thomas 2010; Castillo-Rogez *et al.* 2007; Thomas 2010).

To some, the equatorial position of the ridge and Iapetus’ odd shape suggest a causal relationship. Most current explanations invoke endogenic processes. For example, detailed models of Iapetus’ early thermal evolution suggest that an early epoch of heating due to short-lived ^{26}Al and ^{60}Fe is required to close off primordial porosity in the object while simultaneously allowing it to rapidly de-spin, cool, and lock in a “fossil bulge” indicative of an early faster spin period (Castillo-Rogez *et al.* 2007; Robuchon *et al.* 2010). Recently, Sandwell & Schubert (2010) suggested a new and innovative mechanism for forming the bulge and ridge of Iapetus through contraction of primordial porosity and a thinned equatorial lithosphere. However, only a narrow range of parameters allows both a thick enough lithosphere on Iapetus to support the fossil bulge, while also being sufficiently dissipative to allow Iapetus to de-spin due to Saturn’s influence on solar system timescales.

In these scenarios, the ridge represents a large thrust fault arising from de-spinning. One difficulty faced by these ideas is that the stresses arising from de-spinning at the equator are perpendicular to the orientation required to create an equatorial ridge (Melosh 1977). Other interior processes, such as a convective upwelling (Czechowski and Leliwa-Kopystyński 2008), or convection coupled with tidal dissipation driven by the de-spinning (Roberts and Nimmo 2009) are required to focus and reorient de-spinning stresses on the equator. These latter

models have difficulty reproducing the ridge topography because thermal buoyancy stresses are insufficient to push the ridge to its observed height (see Dombard and Cheng 2008).

Alternatively, the ridge may be exogenic. One leading hypothesis is that the ridge represents a ring system deposited onto Iapetus’ surface (Ip 2006; Dombard *et al.* 2010). This model has the benefit of providing a natural explanation for the mass, orientation, and continuity of the ridge, which present a challenge to endogenic models.

Here we extend this idea to include a satellite that accretes out of the ring system beyond the Roche limit. As we show below, this can significantly aid in the de-spinning of Iapetus. In particular, we hypothesize that:

1) Iapetus suffered a large impact that produced a debris disk similar to what is believed to have formed Earth’s Moon (Canup 2004; Ida *et al.* 1997; Kokubo *et al.* 2000). Like the proto-lunar disk, this disk straddled the Roche radius of Iapetus, and was quickly collisionally damped into a disk. As a result, a satellite accreted beyond the Roche radius, while a particulate disk remained on the inside. Also, the impact left Iapetus spinning with a period ≤ 16 hr, thereby causing the bulge to form.¹

2) Gravitational interactions between the disk and Iapetus’ satellite (hereafter known as the sub-satellite) pushed the disk onto Iapetus’ surface, forming the ridge. As Ip (2006) first suggested, a collisionally damped disk, similar to Saturn’s rings, will produce a linear feature precisely located along the equator. Thus, it naturally explains the most puzzling properties of the ridge system. The impact velocity of the disk particles would have been only ~ 300 m s^{-1} and mainly tangential to the surface, so it is reasonable to assume that they would not have formed craters, but instead piled up on the surface.

3) Tidal interactions between Iapetus and the sub-satellite led to the de-spinning of Iapetus as the sub-satellite’s orbit expanded. Eventually, the sub-satellite evolved far enough from Iapetus that Saturn stripped it away. Iapetus was partially de-spun and continued de-spinning under the influence of Saturn. Finally, the sub-satellite was either accreted by one of Saturn’s regular satellites (most likely Iapetus itself) or was ejected to heliocentric orbit (cf. §5). The end-state is a de-spun Iapetus that has both a bulge and a ridge. Faster de-spinning aided by the presence of a sub-satellite likely relaxes constraints on the early thermal evolution of Iapetus determined by prior works (Castillo-Rogez *et al.* 2010; Robuchon *et al.* 2010).

Because the results of one part of our story can be required by other parts, we begin our discussion in the middle and first find, through numerical simulations, the critical distance

¹It is important to note that the impact that we envision is in a region of parameter space that has yet to be studied. Such an investigation requires sophisticated hydrodynamic simulations and thus is beyond the scope of this paper. We leave it for future work. We emphasize, however, that the general geometry we envision has been seen in many hydrodynamic simulations of giant impacts (e.g., Canup 2004), so we believe that our assumed initial configuration is reasonable.

(a_{st}) at which a sub-satellite of Iapetus will get stripped by Saturn. Knowing this distance, we integrate the equations governing the tidal interactions between both Saturn and Iapetus, and between Iapetus and the sub-satellite, to estimate limits on the mass of the sub-satellite. We then study the fate of the sub-satellite once it was stripped away from Iapetus by Saturn. Finally, using crater scaling relations we reconcile a sub-satellite impact with the topography of Iapetus.

2. Satellites Stripped by Saturn

The distance at which a satellite of Iapetus becomes unstable is important for calculating tidal evolution timescales. In systems containing the Sun, a planet, and a satellite, prograde satellites are not expected to be stable beyond $\sim R_{\text{H}}/2$, where the Hill radius is defined as $R_{\text{H}} = a(m/3M)^{1/3}$ with a as the planet’s semi-major axis, m as its mass, and M as the total system mass (Hamilton and Burns 1991; Barnes and O’Brien 2002; Nesvorný *et al.* 2003). In our case, Iapetus plays the role of the planet, and Saturn the role of the Sun. However, the tidal evolution timescale depends strongly on semi-major axis (as the $-13/2$ power, Eq. 3) and thus the success of our model depends sensitively on the value of the critical distance, a_{st} . Therefore, we performed a series of numerical simulations to determine a_{st} .

This experiment used the `swift_WHM` integrator (Levison & Duncan 1994; which is based on Wisdom & Holman 1991) to integrate two sets of test particles consisting of 500 objects, each of which were initially on orbits about Iapetus with semi-major axes, a , that ranged from 0.1–0.8 R_{H} . The particles in the first set were initially on circular orbits in the plane of Iapetus’s equator. Particles in the second set had initial eccentricities, e , of 0.1, and inclinations, i , that were uniformly distributed in $\cos(i)$ between $i=0$ and $i=15^\circ$. Saturn is by far the strongest perturber to the Iapetus-centered Kepler orbits and is the main source of the stripping. For completeness, we have also included the Sun and Titan. The effects of the other Saturnian satellites are at least two orders of magnitude smaller than those of Titan and thus can be ignored.

The simulations were performed in an Iapetus-centered frame. The lifetime of particles dropped precipitously beyond 0.4 R_{H} , suggesting that any sub-satellite with a larger semi-major axis would very quickly go into orbit around Saturn (Fig. 1). Thus, we adopt this limit, which is equivalent to 21 R_{I} , in our calculations below.

[Fig. 1. here]

3. Tidal evolution of Iapetus

The de-spinning of Iapetus by Saturn has long been considered problematic, because for nominal $Q/|k_2|$ ($\sim 10^5$), Iapetus should not have de-spun over the age of the solar system

(Peale 1977). Starting with the assumption of constant $Q/|k_2|$, and using the standard de-spinning timescale (Murray & Dermott 1999, eq 4.163),

$$\dot{\Omega}_I = -\text{sign}(\Omega_I - n) \frac{3|k_2|}{2\alpha Q} \frac{m_\eta^2}{m_I(m_\eta + m_I)} \left(\frac{R_I}{a}\right)^3 n^2 \quad (1)$$

where $\alpha \leq 2/5$ is the moment of inertia constant of Iapetus, m_I is its mass, Ω_I is its spin frequency, $|k_2|$ is the magnitude of the k_2 Love number, Q the tidal dissipation factor, m_η is the mass of Saturn, and a and n are the semi-major axis and mean motion of Iapetus. The $|k_2|$ and Q values used throughout are for Iapetus only. For the tidal interaction between Iapetus and Saturn, $\Omega_I > n$, so the effect is always to decrease the spin of Iapetus.

For these simple assumptions, the de-spinning from 16 h to a rate synchronous with the orbital period, 79.3 days, takes $3.6 \times 10^5 (Q/|k_2|)$ years, nominally 36 Gyr, for a density $\rho = 1 \text{ g cm}^{-3}$. Using detailed geophysical models, Castillo-Rogez et al. (2007) and Robuchon et al. (2010) showed Saturn can de-spin Iapetus on solar system timescales, although only for a narrow range of thermal histories. Our goal here is to investigate how the addition of the sub-satellite affects the de-spinning times.

Given that detailed models of Castillo-Rogez et al. (2007) and Robuchon et al. (2010) used different methods, and that we are only interested in how the de-spinning timescale changes with the addition of a satellite, we take a simple approach of integrating a modified version of Eq. 1. Our first adjustment is to remove the assumption of constant $Q/|k_2|$. This ratio is dependent on the tidal frequency, $(\Omega - n)$, and accounts for the manner in which a material or body reacts to tidal stresses. We start with a model of Iapetus consisting of a time-invariant 200-km thick lithosphere with a Maxwell viscoelastic rheology with rigidity $\mu = 3.6 \times 10^9 \text{ Pa}$ and viscosity $\eta = 10^{22} \text{ Pa s}$, which is strong enough to support the equatorial bulge and ridge Castillo-Rogez *et al.* (2007), overlying a mixed ice/rock mantle with a lower viscosity, representative of an interior warmed by radiogenic heating. We performed two types of simulations. In the first, the viscosity of the mantle is held constant with time and has values from $\eta = 10^{15} - 10^{18} \text{ Pa s}$ (typical for the interior of an icy satellite at 240 – 270 K). In the second, we allow η of the inner ice/rock mantle to vary according to the thermal evolution models in Castillo-Rogez et al. (2007) and Robuchon et al. (2010). In particular, we employ the LLRI model of Castillo-Rogez et al. (2007), and the 0.04 and 72 ppb ^{26}Al cases from Robuchon et al. (2010). Love numbers are calculated for a spherically symmetric, uniform-density Iapetus using the SatStress software package (Wahr et al. 2009). We calculate the Love number k_2 (which is a complex number for a viscoelastic body, see Wahr et al., 2009 for discussion) and estimate $Q/|k_2| = 1/\text{Im}(k_2)$ (Segatz et al. 1988). The values of $Q/|k_2|$ vary over an order of magnitude for each value of η for the important range of tidal frequencies.

An integration of equation (1) was performed using a Bulirsch-Stoer integrator for times up to 100 Gyr, incorporating the frequency dependent $Q/|k_2|$ for different internal viscosities

which, in turn, is a function of temperature. Without the sub-satellite, the time for Iapetus to reach synchronous rotation ranged between 5×10^8 (fixed $\eta = 10^{15}$ Pa s) to 2×10^{12} years (0.04 ppb ^{26}Al case from Robuchon et al. 2010). We describe an investigation of the effect that a sub-satellite could have on the spin of Iapetus in the next subsection.

3.1. Tidal interaction with a sub-satellite

The sub-satellite raises a tidal bulge on Iapetus, causing Iapetus to de-spin and the sub-satellite’s orbit to change. The change in spin rate for Iapetus due to a sub-satellite is (Murray & Dermott 1999, eq. 4.161),

$$\dot{\Omega}_{\text{I}} = -\text{sign}(\Omega_{\text{I}} - n) \frac{3|k_2|}{2\alpha Q} \frac{m_{\text{ss}}^2}{m_{\text{I}}(m_{\text{I}} + m_{\text{ss}})} \left(\frac{R_{\text{I}}}{a}\right)^3 n^2 \quad (2)$$

and, the change in the satellite’s orbit by (Murray & Dermott 1999, eq. 4.162),

$$\dot{a} = \text{sign}(\Omega_{\text{I}} - n) \frac{3|k_2|}{2\alpha Q} \frac{m_{\text{ss}}}{m_{\text{I}}} \left(\frac{R_{\text{I}}}{a}\right)^5 na. \quad (3)$$

Together Eqs. 2 and 3 describe the interaction between the sub-satellite and Iapetus, where m_{ss} is the mass of the sub-satellite. The term $\text{sign}(\Omega_{\text{I}} - n)$ is of great importance, determining whether the satellite evolves outward while decreasing the spin of Iapetus, or inwards while increasing the spin of Iapetus. At semi-major axis $a_{\text{sync}} = (G(m_{\text{I}} + m_{\text{ss}})/\Omega_{\text{I}}^2)^{3/2}$, $\Omega_{\text{I}} = n$, representing a synchronous state. If the sub-satellite has $a < a_{\text{sync}}$, it evolves inwards; if $a > a_{\text{sync}}$, it evolves outwards. Saturn is gradually decreasing the rotation rate of Iapetus, and thus the synchronous limit slowly grows larger, possibly catching and overtaking a slowly evolving sub-satellite. The orbital period of a sub-satellite at $21 R_{\text{I}}$, the distance at which we consider a satellite stripped by Saturn, is ~ 12.8 days. Thus, if Iapetus is de-spun to a period of 12.8 days before the sub-satellite reaches $21 R_{\text{I}}$, it will be caught by the expanding synchronous limit.

For the integrations of the sub-satellite’s tidal evolution, the sub-satellite’s mass is used as a free parameter, while the starting semi-major axis is set to $3 R_{\text{I}}$. This distance is derived from the expected origin of the sub-satellite accreting from an impact-caused debris disk encircling Iapetus (Ida *et al.* 1997; Kokubo *et al.* 2000). However, tidal evolution timescales for a sub-satellite are largely insensitive to the initial semi-major axis, so this starting point only needs to be beyond the synchronous limit for the model to be accurate. With a rotation period of 16 h for Iapetus, a_{sync} would have been $2.94 R_{\text{I}}$, which is outside the Roche limit defined to be at $r_{\text{roche}} = 2.46 R_{\text{I}}(\rho_{\text{I}}/\rho_{\text{ss}})^{1/3} \approx 2.53 R_{\text{I}}$ for $\rho_{\text{ss}} = 1 \text{ g cm}^{-3}$. Thus, a satellite forming at $3.0 R_{\text{I}}$ would be above the synchronous limit and destined, initially, to evolve outward due to tidal interaction with Iapetus.

Equations (2) and (3) were then integrated with equation (1), to follow the evolution of the spin of Iapetus due to Saturn and the sub-satellite. We studied the geophysical models for Iapetus described in the last section, along with sub-satellites with mass ratios, $q \equiv m_{ss}/m_I$, between 0.0001 and 0.04. We summarize the suite of simulations in Fig. 2, showing the time of de-spinning for Iapetus and the time at which the sub-satellite is stripped by Saturn or tidally evolves back to re-impact Iapetus. We present the data scaled to the de-spinning time due to Saturn alone to highlight the effect of the sub-satellite in accelerating the tidal evolution of the system. The fate of the system, in regards to the escape or re-impact of the sub-satellite and the de-spinning time of Iapetus, are separated into three distinct classes of outcomes based on q .

3.1.1. Synchronous lock and re-impact: $q > 0.021$

Above a mass ratio $q > 0.021$, the sub-satellite does not reach a_{st} before becoming synchronous with the spin of Iapetus (see Fig. 3a). With both the sub-satellite and Saturn working to slow the spin of Iapetus, the synchronous limit grows to $21 R_I$ before the sub-satellite evolves to that semi-major axis. This result only varies mildly for the different geophysical models of Iapetus, as all three timescales depend linearly on $Q/|k_2|$; therefore, the re-impact outcome only depends on mass ratio. However, the time to reach this outcome ranges from 10^{12} yr for the Robuchon et al. (2010) models to 10^9 yr for the Castillo-Rogez et al. (2007) LLRI model.

Upon reaching synchronous rotation, the evolution does not stop because Saturn is still tidally interacting with Iapetus. As Saturn continues to slow the spin rate of Iapetus, the synchronous limit moves beyond the sub-satellite, which then begins to tidally evolve inwards. The sub-satellite is doomed to evolve inwards and hit Iapetus. Given that the sub-satellite started at $3 R_I$ and finishes by impacting Iapetus, it makes a net contribution to the angular momentum of Iapetus, and so it is spinning faster than if the sub-satellite were never there. Thus, the de-spinning of Iapetus (after re-impact) finishes later than it would have by Saturn tides alone (see Fig. 3a).

3.1.2. Satellite is stripped: $0.006 < q < 0.021$

For $0.006 < q < 0.021$, the sub-satellite evolves to $21 R_I$ and is stripped by Saturn before attaining a synchronous orbit. As it moves out, the sub-satellite carries away angular momentum from Iapetus, allowing it to rapidly de-spin. This angular momentum is then removed from the Iapetus system when the sub-satellite is stripped.

The sample evolution for a system with a constant $\eta = 10^{16}$ Pa s and $q = 0.018$ (Fig. 3b) shows that the sub-satellite reaches an orbital period of ~ 12 days ($a = 21 R_I$) before Iapetus

reaches that spin period. It is important to note that the sub-satellite does not totally de-spin Iapetus. Instead, it slows Iapetus down enough that Saturnian tides (which are faster because $Q/|k_2|$ is a decreasing function of the spin rate) can finish the job. For all but one (see §3.1.4) of our geophysical models, the sub-satellite can de-spin Iapetus an order of magnitude faster than it is when de-spun by Saturn alone. This order of magnitude difference means that Iapetus could have de-spun in 500 Myr, for situations that would otherwise require the age of the solar system.

3.1.3. *Slow evolution of a small satellite: $q < 0.006$*

The tidal evolution timescale of the sub-satellite’s orbit expansion depends on q , and for smaller mass ratios, the evolution takes longer. Below $q < 0.006$, the de-spinning of Iapetus due to Saturn is fast enough that the location of synchronous rotation sweeps past the sub-satellite (see Fig. 3c). After this occurs, the sub-satellite is then below the synchronous limit and doomed to evolve back in towards Iapetus. In this scenario, the evolution of the sub-satellite back to the surface of Iapetus takes longer than it takes for Iapetus to de-spin.

Iapetus de-spins faster than Saturn otherwise could do alone. In this case, however, the relevant time constraint becomes the sub-satellite impact time (the small open symbols in Fig. 2) rather than the de-spinning time because we currently do not see a satellite. We find that sub-satellite impact time can be shorter than the de-spinning time for $q > 0.003$. However, it should be noted that this dynamical pathway only helps by at most roughly a factor of 2 over Saturn acting alone. In addition, the sub-satellite is likely to tidally disrupt on its way in, forming a second, significantly fresher, ridge. This is probably inconsistent with the ridge’s ancient appearance. Thus, we think that this particular dynamical pathway can probably be ruled out, but we include it for completeness.

3.1.4. *Discussion of sub-satellite tides*

The integrations have bracketed the possible behavior of the Saturn-Iapetus-sub-satellite system. At high and low mass ratios the sub-satellite is doomed to return to re-impact Iapetus, while for $0.006 < q < 0.021$ the sub-satellite is stripped. As Fig. 2 shows, sub-satellites with masses between $0.005 < q < 0.021$ decrease the despinning time over that of Saturn alone. This effect can be as large as a factor of 10 for $q \sim 0.02$. Consistent with prior work, we find that a low-viscosity interior (presumably warmed by radiogenic heating) is required to despin Iapetus over solar system history. We find that the age of the despinning event with and without a sub-satellite are similar if the thermal evolution of Iapetus follows the LLRI model of Castillo-Rogez et al. (2007). In this case, Iapetus’ interior heats slowly during the first Gyr of its history. When the interior is warmed close to the melting point, tides drive rapid despinning. The presence of the sub-satellite can significantly shorten

this period of time, but because the de-spinning time is short irrespective of whether the sub-satellite is present, it does not significantly alter the time in solar system history when Iapetus is de-spun.

4. The ridge and sub-satellite formation

Given the sub-satellite masses which can assist in de-spinning Iapetus, and estimates on the mass of the equatorial ridge, a constraint can be placed on the amount of mass placed into orbit by the original disk-forming impact. The ring of debris which collapses to form the ridge must do so rapidly, as a ring is not currently observed, and the ridge is one of the oldest features on the surface of Iapetus (Giese et al. 2008).

4.1. Ridge mass

The ridge has an unknown mass due to incomplete imaging and significant damage from cratering. Ip (2006) estimated its mass assuming that it had, at one time, completely encircled the equator with a height of 20 km and width of 50 km, $m_{\text{ridge}} = 2 \times \pi \times R_{\text{I}} \times 20 \text{ km} \times 50 \text{ km}$ with a density of 1 g cm^{-3} equals a mass of 4.4×10^{21} grams (Ip 2006 used a radius of 713 km for this mass estimate). Giese et al. (2008) found a maximum height of 13 km in Digital Terrain Models (DTM) models, though the shape model maximum height was 20 km. Comparing the dimensions given by Ip (2006) with the profiles in Giese et al. (2008), we set a lower limit by taking a factor of two in both vertical and horizontal extent and assuming that the cross section is a triangle rather than a rectangle, yielding an estimate ~ 8 times lower, 5.5×10^{20} grams (where we use a radius of 746 km). However, Castillo-Rogez et al. (2007) quote ridge dimensions of 18 km by 200 km over a length of 1600 km, which yields a mass of 3×10^{21} grams, similar to the Ip (2006) estimate. Profiles from the DTM model (Giese et al. 2008; Fig. 5) do not show a recognizable base greater than 50 km for 10 different profiles across the ridge and no elevations greater than ~ 13 km, making this a very high estimate.

We assume that the ridge consists of ring material that lands on the surface of Iapetus, accounting for the equatorial location. Given a ring of material interior to the Roche limit, there are two ways for it to land on the surface of Iapetus: the ring can tidally evolve down to the surface, or it can be pushed there by the newly formed sub-satellite. For reasons discussed below, we focus on the latter.

4.2. Sub-satellite and ring interaction

The tidal evolution of the ring down to the surface of Iapetus requires that the material be inside the synchronous rotation height. As described above, the synchronous height for a rotation period of 16 h is at $a = 2.94 R_I$, which is exterior to the Roche limit at $r_{\text{roche}} = 2.53 R_I$ for $\rho_{\text{ss}} = 1 \text{ g cm}^{-3}$. The ring material evolves due to tides with Iapetus and the sub-satellite that accretes beyond the Roche limit. By comparing our estimates for the sub-satellite (§3.1) to those of the ridge (§4.1), we find that the sub-satellite is more massive than the ridge for the entire range of sub-satellite masses that assist in de-spinning. In this case, the ring spreading timescale is the time it takes a particle to random walk across a distance r Goldreich and Tremaine (1982),

$$t_{\text{spread}} = (191 \text{ yr}) \left(\frac{5600 \text{ g cm}^{-2}}{\Sigma} \right) \left(\frac{150 \text{ km}}{R_{\text{ss}}} \right)^3 \left| \frac{a_{\text{ss}} - r}{566 \text{ km}} \right|^3, \quad (4)$$

where Σ is the surface density of the ring, and R_{ss} and a_{ss} are the radius and the semi-major axis of the sub-satellite, respectively. The surface density (Σ) of the ring is simply the ridge mass spread over the region interior to the Roche limit, $\sim 5.6\text{--}46.4 \times 10^3 \text{ g cm}^{-2}$. The possible range of sub-satellite masses is equivalent to the mass of a single body of radius, R_{ss} , of $\sim 131\text{--}211 \text{ km}$ for a density of 1 g cm^{-3} (or $155\text{--}251 \text{ km}$ for $\rho_{\text{ss}}=0.6 \text{ g cm}^{-3}$). The semi-major axis of the sub-satellite is likely to be $1.3 R_{\text{roche}}$ initially (Kokubo *et al.* 2000), and so the range of possible times for the spreading of the ring is 9–286 years. Thus, even with many conservative approximations, this timescale is many orders of magnitude shorter than other timescales in the problem.

For the sub-satellite masses of interest, the effect of the ring on the sub-satellite would be dwarfed by the much larger effect of Iapetus’s tides.

5. Impact scenarios

In the vast majority of situations in which the addition of a sub-satellite aids de-spinning, the sub-satellite is stripped from its orbit around Iapetus. In these cases the stripped sub-satellite will still be bound in the Saturnian system, at least initially. In this section, we determine the possible fates for these objects and ask what effect this will have on Iapetus.

5.1. The dynamical fate of a stripped sub-satellite

To determine the probability of impact by a stripped sub-satellite we performed a numerical N -body experiment consisting of the orbital evolution of 50 massless test particles initially in orbit around Iapetus. We used SyMBA, a symplectic code which is capable of handling close encounters Duncan *et al.* (1998). The simulations included Titan, Hyperion,

Iapetus, and Phoebe. Particles were stopped if they hit a satellite, crossed Titan’s orbit, became unbound from Saturn, or reached a distance of 0.4 AU from Saturn (roughly its Hill radius). The particles’ initial semi-major axes ranged from 0.4 to 0.8 R_H ($19\text{--}38R_I$) with eccentricities of 0.1. The particles’ inclinations were between 0° and 15° degrees with respect to Saturn’s equator.

After 6 Myr only 1 particle remained in orbit around Iapetus, while 3 particles hit Iapetus before becoming unbound. The remaining 46 particles became unbound from Iapetus, entering orbit about Saturn. These are the objects of interest here because our goal is to determine the fate of a sub-satellite *once* it becomes unbound. Five of them were ejected from the Saturn system by the satellites (entering heliocentric orbit). The remaining 41 objects impacted Iapetus — none hit Titan, Hyperion, or Phoebe. Thus, a stripped sub-satellite has a roughly $41/46 \sim 90\%$ chance of ending its existence by returning from orbit about Saturn and colliding with Iapetus. This fact means that we must consider the effects of such an impact in our scenario.

5.2. Angular Momentum Budget

In cases in which the stripped sub-satellite re-impacts Iapetus, we must consider the angular momentum it imparts. If the resulting spin rate is too fast it will cancel any advantage that was originally gained by the presence of the sub-satellite. We assume that our scenario is still viable if, after the impact, $\Omega_I < \Omega^* = 2 \times 10^{-5}$, where Ω_I is the spin frequency of Iapetus. For spin rates $< \Omega^*$, corresponding to spin periods greater than ~ 4 days, the de-spinning time after the impact will be less than ~ 100 Myr for $\eta=10^{16}$ Pa s.

Assuming the sub-satellite is accreted completely, the magnitude of the angular momentum brought in by the sub-satellite is $H = m_{ss}v_\infty b$, where v_∞ is the satellite’s velocity with respect to Iapetus at “infinity”, and b is the impact parameter. Assuming that Iapetus’s pre-impact rotation is slow, we find that $\Omega_I < \Omega^*$ requires that $b < b^* \equiv 2R_I^2\Omega^*/5qv_\infty$. The maximum value of b that allows a collision with Iapetus is $b_{\max}^2 = R_I^2[1 + (v_{\text{esc}}/v_\infty)^2]$, where v_{esc} is Iapetus’ surface escape speed. If $b^* > b_{\max}$, all impacts leave Iapetus spinning more slowly than Ω^* ; otherwise the probability P that Iapetus will have $\Omega_I < \Omega^*$ (and thus our scenario will remain viable) is $(b^*/b_{\max})^2 = (2R_I\Omega^*/5qv)^2$, where v is the impact speed and we have used $v^2 = v_{\text{esc}}^2 + v_\infty^2$.

In §3.1, we found that satellites with $0.005 < q < 0.021$ were most effective in de-spinning Iapetus. Most impacts occurred at velocities near the escape speed of Iapetus, 0.58 km/s. At that speed, $P = 1$ for $q < 0.0103$ and $P = (0.0103/q)^2$ for $0.0103 < q < 0.021$. Thus, the lower-mass sub-satellites never produce spin rates faster than Ω^* , while sub-satellites with $q = 0.0146$ yield viable scenarios 50% of the time. We therefore conclude that the re-impact of the sub-satellite can be consistent with Iapetus’s spin state.

5.3. Linking basins to the possible sub-satellite impact

A large complex crater or basin will form if the sub-satellite were to impact Iapetus. In this section, we estimate the size of the impactors needed to produce the basins observed on Iapetus today and compare them to the size of the sub-satellite. Zahnle et al. (2003) estimate the diameter, D , of the final (collapsed) crater on a mid-sized icy satellite to be

$$D = 21.4 \text{ km} \left(\frac{v}{1 \text{ km/s}} \right)^{0.49} \left(\frac{1 \text{ cm/s}^2}{g} \right)^{0.245} \left(\frac{\rho_i}{\rho} \right)^{0.377} \left(\frac{R_{ss}}{1 \text{ km}} \right)^{0.885}, \quad (5)$$

where v is the normal component of the impact velocity, g is the surface gravity of the target, ρ is the density of the target, and ρ_i is the density of the impactor. This equation assumes that the incidence angle of the impact, measured from the normal to the target, is 45° . If we substitute $g = 22.3 \text{ cm s}^{-2}$ for Iapetus, $\rho_i = \rho = 1.0 \text{ g cm}^{-3}$, we have

$$D = 589 \text{ km} \left(\frac{v}{1 \text{ km/s}} \right)^{0.49} \left(\frac{R_{ss}}{100 \text{ km}} \right)^{0.885}. \quad (6)$$

Giese et al. (2008) found 7 basins, defined as craters with $D > 300 \text{ km}$, on the leading face of Iapetus. The largest is stated to have $D = 800 \text{ km}$. The Gazetteer of Planetary Nomenclature (<http://planetarynames.wr.usgs.gov/>) lists 5 basins on Iapetus, with the largest, Turgis, 580 km in diameter.

In our scenario, one of Iapetus’s basins may have been created by our escaped sub-satellite when it returns to meet its maker. In our simulations in §5.1, we find that the impact would likely occur at a velocity near Iapetus’s escape velocity, 0.58 km/s ; however, there is about a 10% chance that the impact speed would exceed 2 km/s . At 2 km/s , Eq. (6) indicates that $300 - 800 \text{ km}$ basins are produced by impactors with radii between 32 and 96 km . At the more likely speed of 0.58 km/s , the corresponding impactor radii are 64 and 193 km . Recall that in §4.2, we found that our hypothetical sub-satellite should have radii between 131 and 211 km for these densities. The ranges vary slightly for a sub-satellite of only 0.6 g cm^{-3} with impactors between $40-120 \text{ km}$ at 2 km/s and $80-241 \text{ km}$ at 0.58 km/s , where the hypothetical sub-satellite at this density would have a radii between $155-251 \text{ km}$. Therefore, it is quite possible that one of the observed basins was caused by our hypothetical sub-satellite.

These calculations are highly uncertain because numerical simulations at the relevant scales and velocities have not, to our knowledge, been performed for icy targets. In particular, scaling relations in the literature, such as the Schmidt-Housen scaling we used above, are generally based on field data or simulations of hypervelocity impacts, i.e., impacts at velocities large compared with the speed of sound in the target, which is about 3 km/s for non-porous ice. Impacts by Iapetus’s putative sub-satellite would have occurred at lower speeds. Furthermore, experiments and simulations generally deal with impactors that are much smaller than their targets. This condition is only marginally satisfied at typical speeds

for the impacting sub-satellite in our scenario. Thus, the values we quote for the sub-satellite’s size should be viewed as rough estimates. However, the calculations do support the possibility of basin formation caused by the impacting sub-satellite.

6. Discussion and conclusions

We have explored the scenario in which a sub-satellite forms from an impact-generated debris disk around Iapetus following an impact. The remains of the disk fall to the surface of Iapetus to build the observed equatorial ridge, while the tidal evolution of the sub-satellite assists in de-spinning Iapetus. We find that this scenario can significantly shorten Iapetus’s tidal de-spinning time if the mass ratio between the sub-satellite and Iapetus, q , is between 0.005 and 0.021. These results suggest that the presence of a sub-satellite can potentially loosen constraints on the geophysical history of Iapetus that have been implied by the timing and duration of despinning. The full implications of our results, however, cannot be realized until the sub-satellite scenario is investigated using a detailed thermal evolution model such as those described in prior works (e.g. Castillo-Rogez et al. (2007); Robuchon et al. (2010)).

Iapetus has been of great interest due to its extremely old surface that records the cratering history of the outer solar system. Prior scenarios require that the ridge form after an epoch of early heating to de-spin Iapetus that drive the timing and duration of resurfacing (Castillo-Rogez et al. (2007); Robuchon et al. (2010)). In our model, the ridge forms only a few hundred years after the impact, and therefore the ridge is quite old. This matches the qualitative assessment that the ridge is one of the oldest features on the surface, along with the 800-km basin (Giese *et al.* 2008). Some of the sub-satellite evolutionary scenarios presented here end with a re-impact, requiring an associated basin forming much later.

The ridge is only seen to extend roughly 110° around Iapetus. This could be the result of its extreme age — much of it could have been destroyed by subsequent cratering. Thus, it is still unclear whether the ridge extends for the full extent of the equatorial circumference, but an infalling ring would preferentially deposit material on global topographic high terrain. Indeed, a ring that extends only 110° in longitude could result if the center-of-figure of Iapetus were offset from its center-of-mass as is seen on the Moon (see Araki *et al.* 2009, and references therein).

The stripped sub-satellite mass range, described above, corresponds to bodies with radii of between roughly 130 and 210 km (assuming $\rho_I = 1 \text{ g cm}^{-3}$), not all of which are below the estimated radius, ~ 190 km, of the largest allowable impactor given the basins on Iapetus. This limiting size corresponds to a mass ratio $q = 0.015$. We arrive at a similar upper limit when considering the angular momentum of the impact. Thus, to account for the impact of the secondary, the mass ratio range $0.006 < q < 0.015$ is required. As seen in Fig. 2, the sub-satellites are stripped on very similar timescales to the de-spinning of Iapetus. Thus, a sub-satellite returning to form a basin on Iapetus would do so after the ridge formed. This

younger basin caused by the sub-satellite would then be expected to overlie the ridge if it was a near-equatorial impact. Turgis (the 580 km Basin II in Giese et al. 2008) fulfills these requirements as the equatorial ridge appears to stop when intersecting this basin (though there are no profiles presented in Giese et al. 2008 for this region of the surface). This basin would correspond to an impactor with a radius of 140 km, which is only slightly larger than the lower limit estimated above. However, we find this acceptable given the inherent uncertainties in calculating crater sizes. Meanwhile Basin I, the largest at 800 km, appears to have a stratigraphically similar age as the ridge (Giese *et al.* 2008). It is important to note, however, that our simulations predict only $\sim 90\%$ of stripped sub-satellites return to impact, so it is not a certainty that one of the basins is associated with this evolution.

A strength of our hypothesis is that the limits on impactor and sub-satellite masses ($0.005 < q < 0.015$) are in line with the estimated ridge mass and the number of 300–800 km basins. Thus, this work provides a complete story from original to final impact which may explain the ridge, shape, and basin population on Iapetus.

We would like to thank Michelle Kirchoff and David Nesvorný for useful discussions. HFL and KJW are grateful for funding from NASA’s Origins and OPR program. ACB and LD acknowledge support from NASA CDAP grants.

REFERENCES

- Araki, H., S. Tazawa, H. Noda, Y. Ishihara, S. Goossens, S. Sasaki, N. Kawano, I. Kamiya, H. Otake, J. Oberst, and C. Shum 2009. Lunar Global Shape and Polar Topography Derived from Kaguya-LALT Laser Altimetry. *Science* **323**, 897–900.
- Barnes, J. W., and D. P. O’Brien 2002. Stability of Satellites around Close-in Extrasolar Giant Planets. *ApJ* **575**, 1087–1093.
- Canup, R. M. 2004. Simulations of a late lunar-forming impact. *Icarus* **168**, 433–456.
- Castillo-Rogez, J. C., D. L. Matson, C. Sotin, T. V. Johnson, J. I. Lunine, and P. C. Thomas 2007. Iapetus’ geophysics: Rotation rate, shape, and equatorial ridge. *Icarus* **190**, 179–202.
- Czechowski, L., and J. Leliwa-Kopystyński 2008. The Iapetus’s ridge: Possible explanations of its origin. *Advances in Space Research* **42**, 61–69.
- Dombard, A. J., and A. F. Cheng 2008. Constraints on the Evolution of Iapetus from Simulations of its Ridge and Bulge, abstract 2262. In *Lunar and Planetary Science Conf. Abs. XXXIX*, Houston, Tex.

- Dombard, A. J., A. F. Cheng, W. B. McKinnon, and J. P. Kay 2010. The Weirdest Topography in the Outer Solar System: The Ridge on Iapetus and its Possible Formation via Giant Impact (Invited). pp. P31D–01.
- Duncan, M. J., H. F. Levison, and M. H. Lee 1998. A Multiple Time Step Symplectic Algorithm for Integrating Close Encounters. *AJ* **116**, 2067–2077.
- Giese, B., T. Denk, G. Neukum, T. Roatsch, P. Helfenstein, P. C. Thomas, E. P. Turtle, A. McEwen, and C. C. Porco 2008. The topography of Iapetus’ leading side. *Icarus* **193**, 359–371.
- Goldreich, P., and S. Tremaine 1982. The dynamics of planetary rings. *ARA&A* **20**, 249–283.
- Hamilton, D. P., and J. A. Burns 1991. Orbital stability zones about asteroids. *Icarus* **92**, 118–131.
- Ida, S., R. M. Canup, and G. R. Stewart 1997. Lunar accretion from an impact-generated disk. *Nature* **389**, 353–357.
- Ip, W.-H. 2006. On a ring origin of the equatorial ridge of Iapetus. *Geophys. Res. Lett.* **33**, L16203.
- Jacobson, R. A., P. G. Antreasian, J. J. Bordi, K. E. Criddle, R. Ionasescu, J. B. Jones, R. A. Mackenzie, M. C. Meek, D. Parcher, F. J. Pelletier, W. M. Owen, Jr., D. C. Roth, I. M. Roundhill, and J. R. Stauch 2006. The Gravity Field of the Saturnian System from Satellite Observations and Spacecraft Tracking Data. *AJ* **132**, 2520–2526.
- Kokubo, E., S. Ida, and J. Makino 2000. Evolution of a Circumterrestrial Disk and Formation of a Single Moon. *Icarus* **148**, 419–436.
- Levison, H. F., and M. J. Duncan 1994. The long-term dynamical behavior of short-period comets. *Icarus* **108**, 18–36.
- Melosh, H. J. 1977. Global tectonics of a despun planet. *Icarus* **31**, 221–243.
- Murray, C. D., and S. F. Dermott 1999. *Solar System Dynamics*. New York: Cambridge University Press.
- Nesvorný, D., J. L. A. Alvarelos, L. Dones, and H. F. Levison 2003. Orbital and Collisional Evolution of the Irregular Satellites. *AJ* **126**, 398–429.
- Peale, S. J. 1977. Rotation histories of the natural satellites. In J. A. Burns (Ed.), *IAU Colloq. 28: Planetary Satellites*, pp. 87–111.
- Porco, C. C., et al. 2005. Cassini Imaging Science: Initial Results on Phoebe and Iapetus. *Science* **307**, 1237–1242.

- Roberts, J. H., and F. Nimmo 2009. Tidal Dissipation Due to Despinning and the Equatorial Ridge on Iapetus. In *Lunar and Planetary Institute Science Conference Abstracts*, Volume 40 of *Lunar and Planetary Institute Science Conference Abstracts*, pp. 1927.
- Robuchon, G., G. Choblet, G. Tobie, O. Čadek, C. Sotin, and O. Grasset 2010. Coupling of thermal evolution and despinning of early Iapetus. *Icarus* **207**, 959–971.
- Sandwell, D., and G. Schubert 2010. A contraction model for the flattening and equatorial ridge of Iapetus. *Icarus* **210**, 817–822.
- Segatz, M., T. Spohn, M. N. Ross, and G. Schubert 1988. Tidal Dissipation, Surface Heat Flow, and Figure of Viscoelastic Models of Io. *Icarus* **75**, 187–206.
- Spencer, J. R., and T. Denk 2010. Formation of Iapetus’ Extreme Albedo Dichotomy by Exogenically Triggered Thermal Ice Migration. *Science* **327**, 432–.
- Thomas, P. C. 2010. Sizes, shapes, and derived properties of the saturnian satellites after the Cassini nominal mission. *Icarus* **208**, 395–401.
- Wahr, J., Z. A. Selvans, M. E. Mullen, A. C. Barr, G. C. Collins, M. M. Selvans, and R. T. Pappalardo 2009. Modeling stresses on satellites due to nonsynchronous rotation and orbital eccentricity using gravitational potential theory. *Icarus* **200**, 188–206.
- Wisdom, J., and M. Holman 1991. Symplectic maps for the n-body problem. *AJ* **102**, 1528–1538.
- Zahnle, K., P. M. Schenk, and H. F. Levison 2003. Cratering rates in the outer solar system. *Icarus* **163**, 263–289.

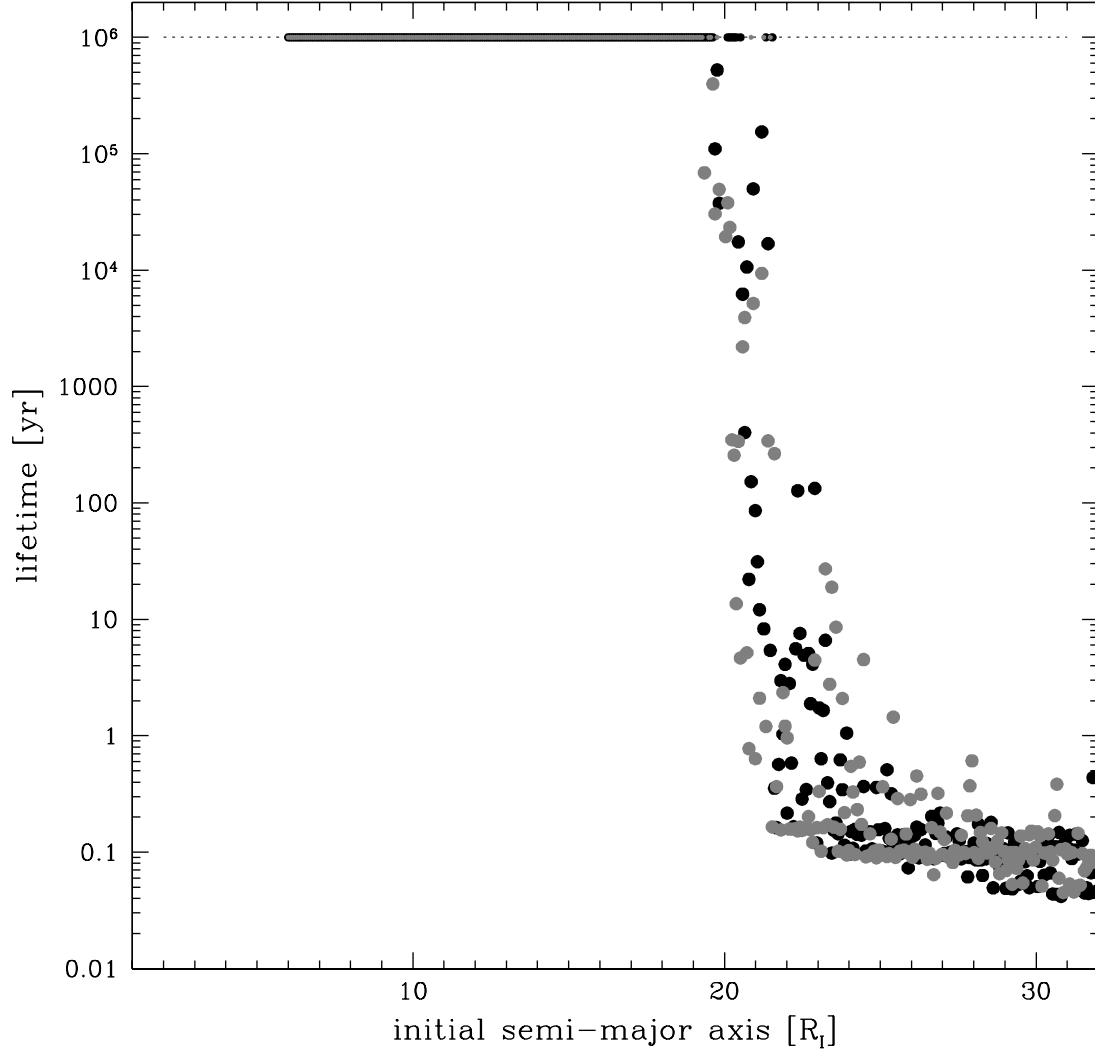


Fig. 1.— The lifetime of each test particle is plotted as a function of their initial semimajor axis for two different initial eccentricities (black) 0.1 and (gray) 0.0. The simulations lasted for 1 Myr, which is shown as a horizontal line. Symbols for particles which survive for 1 Myr are smaller than those of particles with shorter lifetimes. The lifetime drops precipitously at $a = 21 R_I = 0.44 R_H$.

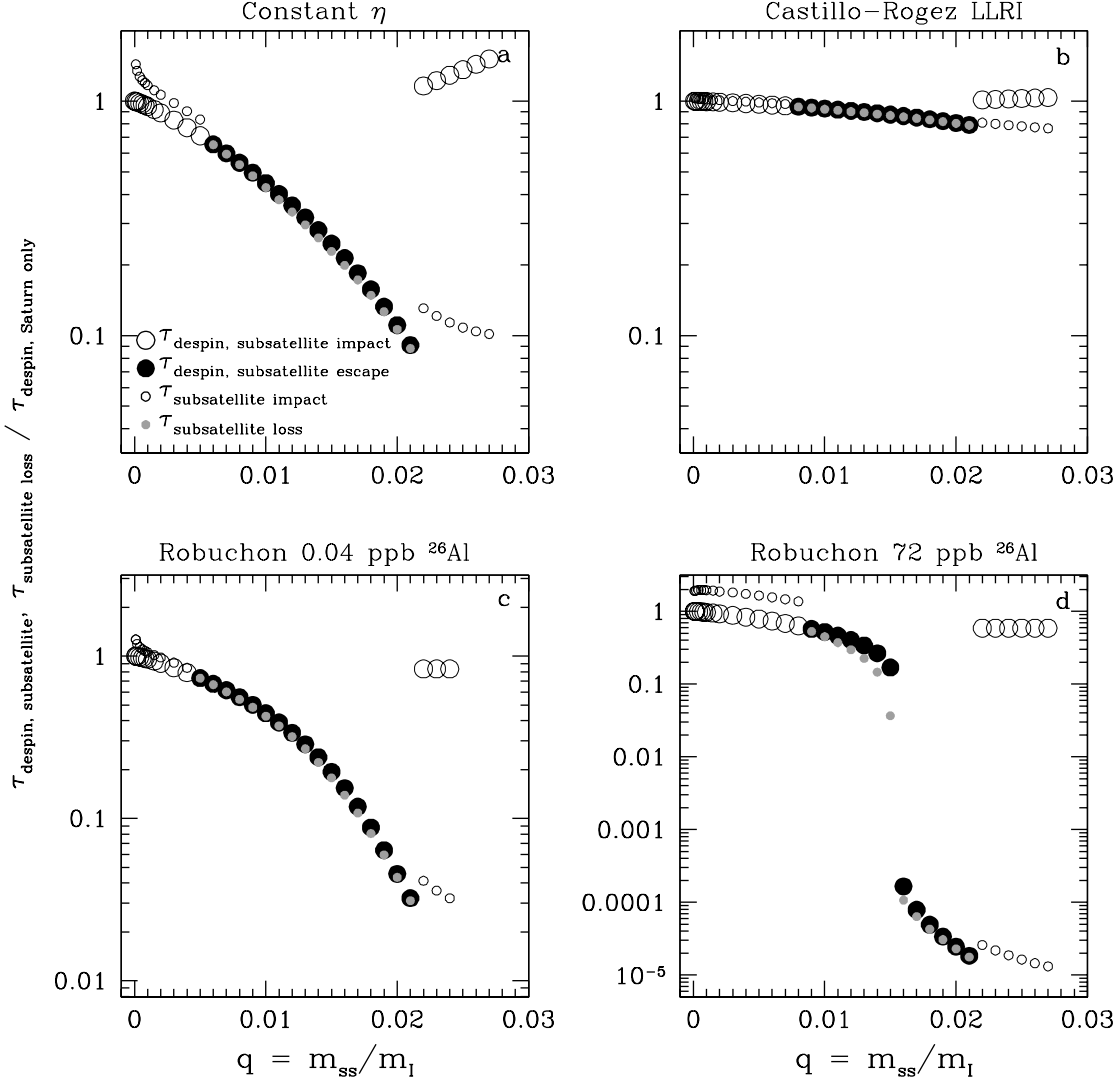


Fig. 2.— Results from the integrations of the despinning of Iapetus, where despinning and sub-satellite stripping/impacting timescales were calculated for different mass ratios q for different internal viscosities η and different internal temperature evolution. The filled symbols are the despinning times for simulations where the sub-satellite is stripped, where the smaller symbol at the same q is the time of stripping. The open symbols are for cases where the sub-satellite evolves back towards Iapetus, and the smaller symbol marks the time of re-impact. The times are normalized to the time it takes Iapetus to de-spin by Saturnian tides alone for each case. Four cases are plotted: (a) constant viscosity, where the results from each constant value of $\eta = 10^{15}$ Pa s, $\eta = 10^{16}$ Pa s, etc. plot on top of each other when normalized to 1.0, (b) the LLRI case from Castillo-Rogez (2007), (c) the 0.04 ppb and (d) 72 ppb ^{26}Al cases from Robuchon et al. (2010).

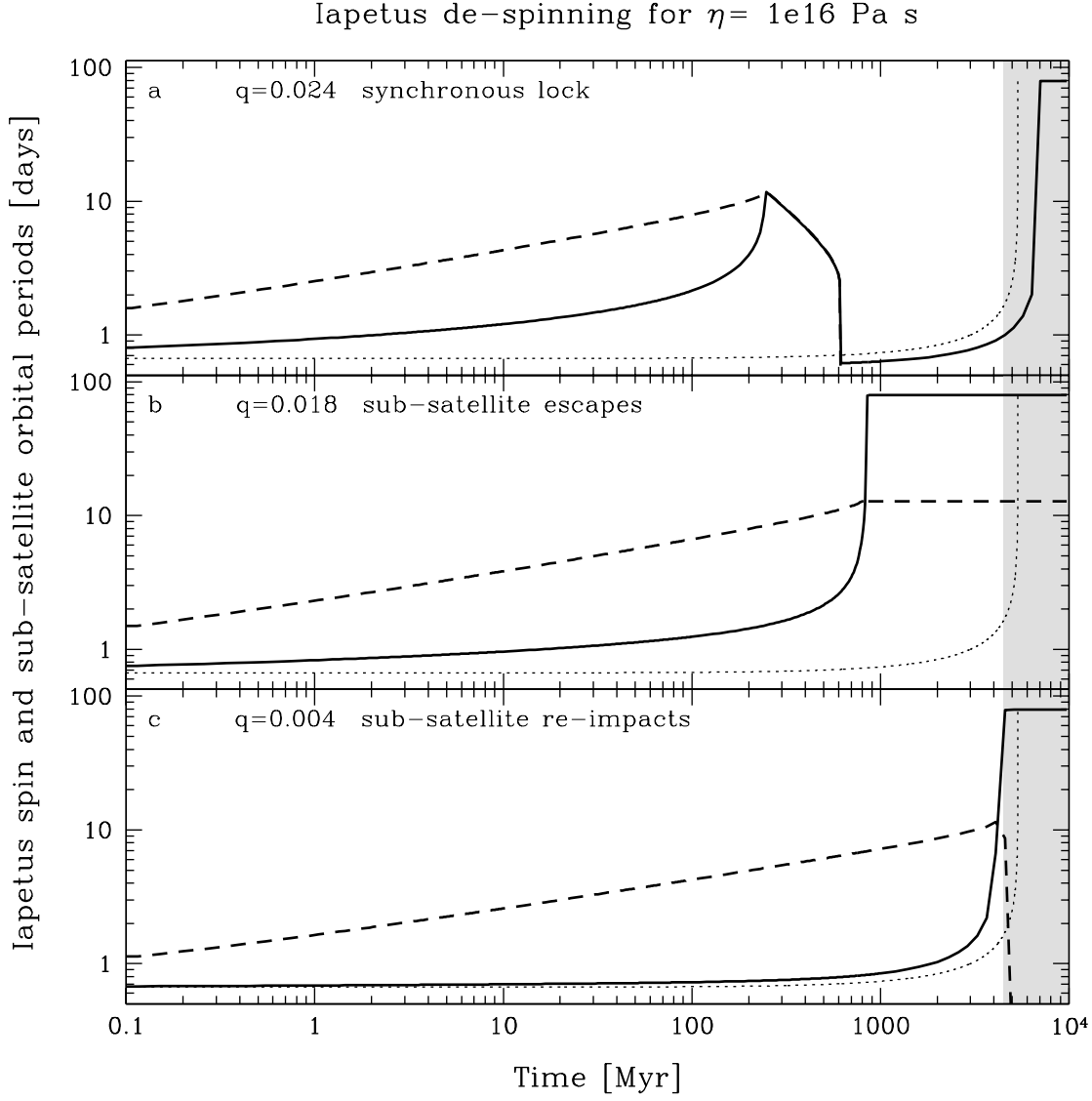


Fig. 3.— Evolution of the spin period of Iapetus (solid line) and orbital period of the sub-satellite (dashed line) as a function of time, for with constant η equal to 10^{16} Pa s and mass ratios of (a) $q = 0.024$, (b) $q = 0.018$ and (c) $q = 0.004$. The dotted line in each panel is the evolution of the spin of Iapetus under the influence of Saturn only, and the shaded region marks the age of the solar system. They illustrate three different outcomes. In case (a) the sub-satellite is too large and eventually is caught in synchronous lock with the rotation of Iapetus. Saturn continues despinning Iapetus, and so the sub-satellite falls below synchronous height, returning to impact Iapetus. Iapetus then despins, again, due to Saturn, and finally reaches a despun state later than had it simply despun due to the effects of Saturn. In case (b) the sub-satellite assists in despinning Iapetus, and is then stripped by Saturn, allowing Iapetus to despin up to $10\times$ faster than by Saturn alone. Finally, in (c), the small sub-satellite’s orbit evolves very slowly, so that Iapetus is despun by Saturn fast enough for the synchronous limit to move beyond the sub-satellite, forcing the sub-satellite to tidally contract its orbit and return to impact Iapetus. For this case the despinning time is similar to that by Saturn’s effect alone.